



Published in final edited form as:

*J Occup Environ Hyg.* 2013 ; 10(3): 109–115. doi:10.1080/15459624.2012.752321.

## Penetration of Fiber Versus Spherical Particles Through Filter Media and Faceseal Leakage of N95 Filtering Facepiece Respirators with Cyclic Flow

Kyungmin Jacob Cho<sup>1</sup>, Leonid Turkevich<sup>2</sup>, Matthew Miller<sup>2,3</sup>, Roy McKay<sup>1</sup>, Sergey A. Grinshpun<sup>1</sup>, KwonChul Ha<sup>4</sup>, and Tiina Reponen<sup>1</sup>

<sup>1</sup>Department of Environmental Health, University of Cincinnati, Cincinnati, Ohio

<sup>2</sup>National Institute for Occupational Safety and Health, Cincinnati, Ohio

<sup>3</sup>Department of Chemical Engineering, University of Cincinnati, Cincinnati, Ohio

<sup>4</sup>Department of Biochemistry & Health Science, Changwon National University, Changwon, Korea

### Abstract

This study investigated differences in penetration between fibers and spherical particles through faceseal leakage of an N95 filtering facepiece respirator. Three cyclic breathing flows were generated corresponding to mean inspiratory flow rates (MIF) of 15, 30, and 85 L/min. Fibers had a mean diameter of 1  $\mu\text{m}$  and a median length of 4.9  $\mu\text{m}$  (calculated aerodynamic diameter,  $d_{ae} = 1.73 \mu\text{m}$ ). Monodisperse polystyrene spheres with a mean physical diameter of 1.01  $\mu\text{m}$  (PSI) and 1.54  $\mu\text{m}$  (PSII) were used for comparison (calculated  $d_{ae} = 1.05$  and 1.58  $\mu\text{m}$ , respectively). Two optical particle counters simultaneously determined concentrations inside and outside the respirator. Geometric means (GMs) for filter penetration of the fibers were 0.06, 0.09, and 0.08% at MIF of 15, 30, and 85 L/min, respectively. Corresponding values for PSI were 0.07, 0.12, and 0.12%. GMs for faceseal penetration of fibers were 0.40, 0.14, and 0.09% at MIF of 15, 30, and 85 L/min, respectively. Corresponding values for PSI were 0.96, 0.41, and 0.17%. Faceseal penetration decreased with increased breathing rate for both types of particles ( $p < 0.001$ ). GMs of filter and faceseal penetration of PSII at an MIF of 30 L/min were 0.14% and 0.36%, respectively. Filter penetration and faceseal penetration of fibers were significantly lower than those of PSI ( $p < 0.001$ ) and PSII ( $p < 0.003$ ). This confirmed that higher penetration of PSI was not due to slightly smaller aerodynamic diameter, indicating that the shape of fibers rather than their calculated mean aerodynamic diameter is a prevailing factor on deposition mechanisms through the tested respirator. In conclusion, faceseal penetration of fibers and spherical particles decreased with increasing breathing rate, which can be explained by increased capture by impaction. Spherical particles had 2.0–2.8 times higher penetration through faceseal leaks and 1.1–1.5 higher penetration through filter media than fibers, which can be attributed to differences in interception losses.

## Keywords

particle shape; protection factor; total inward leakage

---

## INTRODUCTION

Filtration is a simple, versatile, and economical means for collecting aerosol particles of different shapes and sizes. Therefore, aerosol filtration has various applications in diverse fields such as respiratory protection and air cleaning.<sup>(1)</sup> Filtering facepiece respirators (FFRs) are commonly used in a variety of workplaces due to their low price, comfort, ease of use, and efficiency.<sup>(2)</sup> Respirators are typically tested with spherical particles, and little is known about the overall performance of currently used respirators against fibrous particles such as asbestos, fiberglass, and ceramic fibers.

Deposition of aerosol particles on filter media includes a variety of mechanisms, such as diffusion, inertial impaction, and interception. For particles with diameters above 1  $\mu\text{m}$ , the last two mechanisms are most prominent and depend on particle shape and aerodynamic diameter. The aerodynamic behavior of fibrous particles is mostly dependent on the diameter of fiber, with a minor influence of the length.<sup>(3)</sup> However, elongated particles are known to have increased filter collection due to interception compared with spherical particles of the same aerodynamic diameter. One would expect that, similar to the filter media penetration, the particle penetration through face seal leakage should also be affected by the particle length, but there are no data to substantiate this.

Several studies have been conducted on filter penetration of asbestos. Brosseau et al.<sup>(4)</sup> measured filter penetration of amosite (asbestos) through dust/mist respirators under constant and cyclic flows. The fibers had count median diameter (CMD) of 0.2  $\mu\text{m}$  and count median length (CML) of 4.5  $\mu\text{m}$ . They reported an average filter penetration of 0.01–0.1% at a constant flow of 32 L/min and 0.1–0.6% at a sinusoidal cyclic flow of 76 L/min (mean inspiration flow, MIF). Remarkably, one filter type had 60 times higher penetration under the cyclic than under the constant flow. Ortiz et al.<sup>(5)</sup> compared filter penetrations between chrysotile (asbestos) and oil test aerosols (di-(2-ethylhexyl) sebacate, DEHS) through dust/mist respirators. Fibers with lengths over 5  $\mu\text{m}$  were included when calculating the filter penetration; DEHS size was reported as 0.2–0.3  $\mu\text{m}$  without indication of the type of diameter (aerodynamic, physical, or optical). They found lower penetration for asbestos (0–3%) compared with DEHS (0–30%). Cheng et al.<sup>(6)</sup> also compared filter penetration of the DEHS with a mass median aerodynamic diameter of 0.30  $\mu\text{m}$  and three types of asbestos fibers through four different types of respirators: disposable face mask, dust/mist mask, powered respirator, and HEPA filter. The three asbestos types were amosite, crocidolite, and chrysotile, with CMDs 0.18, 0.08, and 0.03  $\mu\text{m}$ , respectively. The corresponding CMLs were 1.19, 0.53, and 0.62  $\mu\text{m}$ . Only high efficiency particulate air (HEPA) filters had similar penetration levels between DEHS particles and the three types of asbestos fibers.<sup>(6)</sup> Filter penetration of asbestos fibers and DEHS particles through the other respirators ranged from below 0.01 to 8.63% and below 0.01 to 15.37%, respectively. Penetrations of amosite and crocidolite through the non-HEPA respirators were lower than those of the DEHS.

In previous studies, overall filter penetrations of different asbestos fibers have been reported with a lack of information on the aerodynamic diameter. It may not be appropriate to directly compare those values with each other and with spherical particles due to the different characteristics of asbestos fibers (length and aerodynamic diameter). Moreover, some studies were conducted before the issuance of new respirator certification regulations that designate filters based on filter efficiency (95, 99, and 100%) and resistance to solid or liquid aerosols (N, R, and P). Most importantly, to our knowledge, none of the previous studies have investigated face-seal penetration of fibrous materials, even though face-seal leakage accounts for most of the particle penetration through respirators.<sup>(7,8)</sup> Thus, the objective of this study was to compare filter and face-seal penetrations of fibrous materials and spherical particles through an N95 filtering facepiece respirator at different cyclic breathing rates.

## METHODS

### Experimental Setup

Total penetration and filter penetration were determined using an experimental setup shown in Figure 1. A manikin wearing an N95 filtering facepiece respirator (FFR) (Pleats Plus, AOSafety; 3M, St. Paul, Minn.) was placed in a walk-in test chamber (volume = 24.3 m<sup>3</sup>). The manikin was connected to a breathing simulator (Koken Ltd., Tokyo, Japan), which generated three sinusoidal breathing flows corresponding to MIF (mean inspiratory flow rate) of 15, 30, and 85 L/min. The breathing simulator generates sinusoidal flow using an electromechanical cylinder connected to two air cylinders, which move back and forth. A HEPA filter was placed between the manikin and the breathing simulator to prevent re-entry of particles into the respirator cavity with the exhalation flow. Challenge aerosols were aerosolized by a Koken nebulizer described in detail in Cho et al.,<sup>(7)</sup> dried by mixing with filtered dry air of 100 L/min, and fed into a <sup>85</sup>K charge neutralizer (3054; TSI Inc., Minneapolis, Minn.) to attain a Boltzmann charge distribution. Three different challenge aerosols were used: fibers and polystyrene particles of two different sizes (PSI and PSII).

Particle concentrations inside and outside the respirator were determined concurrently by two optical particle counters (OPCs, HHPC-6; Hach Company, Loveland, Colo.) in triplicate at each breathing rate. Concentration measured inside the respirator was divided by that measured outside the respirator to calculate penetration (P) in percent:

$$P(\%) = (C_{in}/C_{out}) \times 100 \quad (1)$$

The optical particle counter measured particle number concentrations in five channels: 0.7–1.0, 1.0–2.0, 2.0–3.0, 3.0–5.0, and 5.0–10.0 μm. For every condition, penetration was calculated in 1-min intervals and averaged over 15 min. All concentrations outside the respirator in the chamber were maintained in the range of 28,000–33,000 particles/L during the experiment.

An N95 FFR was partially glued to a manikin face from the cheekbone toward the chin to obtain total penetration comparable to one observed in a field study for human subjects as

previously described.<sup>(7)</sup> The quoted field study was conducted in agricultural environments, and the workplace protection factor was 515 corresponding to mean particle penetration of 0.2%.<sup>(7)</sup> The commercially available manikin (Allen Display) had face width of 109 mm and face length of 121 mm. The respirator used for these experiments is flexible and easily adjustable to the various facial sizes and shapes using the non-adjustable straps. The location of the respirator was marked on the manikin face to ensure repeatable placement location. The length of sealing was 11 cm on both left and right sides of the respirator. A manikin wearing an N95 FFR was placed in the walk-in test chamber and connected to the breathing simulator.

To estimate the fit of the respirator to the manikin, total penetration testing was also conducted using conventional quantitative fit-testing equipment (PortaCount Plus 8020 with an N95 companion 8095; TSI Inc.) using three MIFs. A custom version of the TSI Portacount software was used to obtain “fit factor” values above 200. Testing of fit to the manikin is based on aerosol measurement of charged particles at the nominal particle size of 50 nm,<sup>(9)</sup> whereas the penetration of fibers was assessed in this study using an optical particle counter in the size range of 0.7–10  $\mu\text{m}$ . For the total penetration testing, a Collison nebulizer (BGI Inc., Waltham, Mass.) with NaCl solution intermittently generated challenge aerosols. The challenge aerosols were mixed with filtered dry air of 100 L/min and passed through a <sup>85</sup>K charge neutralizer. Fit test exercise protocols were not used during total penetration testing with the manikin system. At the three MIF values of 15, 30, and 85 L/min, total penetration values measured with the Portacount were, respectively, 0.296%, 0.314%, and 0.282%. These total penetration values correspond to “fit factors” of, respectively, 338, 2315, and 355. Penetration of fibers and PSL particles measured with the partially sealed facepiece represented total penetration ( $P_{\text{total}}$ ). Filter penetration ( $P_{\text{filter}}$ ) was measured separately after the FFR was fully sealed to the manikin face. Face seal penetration ( $P_{\text{face seal}}$ ) was determined by deducting the filter penetration from total penetration at the same breathing rate as shown below.

$$P_{\text{face seal}} = P_{\text{total}} - P_{\text{filter}} \quad (2)$$

### Preparation of Challenge Aerosols

Fibers were prepared in the following manner. Pall glass fiber sheet type A/E (part no. 61638; Pall Life Sciences, Ann Arbor, Mich.) was the starting material. This media consists of entangled uncoated borosilicate glass fibers (of nominal diameter  $d = 1 \mu\text{m}$ ), designed to retain 1- $\mu\text{m}$  particles on filtration. Batches of 24 sheets were cut out to fit into a dye cavity and crushed with a lab press under a pressure of 1 ton for a few seconds. Each batch yields ~ 1.5 g of fiber.

The dry particles were dispersed (at 10 wt.%) in 0.2 wt.% aqueous solution of cetyl trimethylammonium bromide and sonicated; this protocol minimizes particle aggregation. An aliquot of the dispersion was diluted and filtered through a mixed cellulose ester (MCE) filter (Millipore Corp., Billerica, Mass.). The acetone-clarified filter was imaged with an optical microscope at 40 $\times$  (Figure 2 shows a similar filter from the sampled aerosol,

described below). Particle lengths in the generator suspension were measured by Motic software (Motic Images Plus 2.0; Motic Group, Richmond, BC, Canada). For the filtered dispersion, 468 particles were measured. The particle length distribution was reasonably well described by a log-normal distribution (Figure 3a) with a geometric mean length,  $L = 6.7 \mu\text{m}$  and a geometric standard deviation,  $\text{GSD} = 1.9$ . The cumulative length distribution (on a linear scale) is shown in Figure 3b. About 50% of particles were  $>5 \mu\text{m}$  long, and about 92% of particles were  $>3 \mu\text{m}$  long (i.e., had aspect ratio  $>3$  as the mean diameter was  $1 \mu\text{m}$ ).

In the length measurements, the optical microscopy is not sensitive to particles with size  $< 1 \mu\text{m}$ . We did not measure the diameter of particles of this particular sample, but our experience with measuring other samples prepared in this manner from the Pall glass fiber sheets (optical microscopy and TEM) is that  $d \sim 1 \mu\text{m}$  with negligible number of particles outside the range  $0.8 \mu\text{m} < d < 1.2 \mu\text{m}$ . The “mottled” background of the clarified MCE filter (Figure 2) obscures the imaging of particles smaller than  $1 \mu\text{m}$ . Furthermore, fibers oriented perpendicular to the focal plane look like spherical particles in the two-dimensional image.

This dispersion was aerosolized, with the Koken nebulizer, as described above. In a calibration experiment, we waited 30 min to establish a steady state aerosol concentration in the chamber ( $2.4 \times 10^4$  particles/L), as measured by the OPC. We then sampled, again through MCE filters, for 30 min, at a flow rate of 5.0 L/min. Two such filters were collected, acetone clarified, and particle lengths measured. The particle length distribution was distorted from the original log-normal distribution in that the aerosol was depleted of the longer particles (Figure 3a) so that the median length was  $4.85 \mu\text{m}$  (geometric mean particle length =  $4.90 \mu\text{m}$ ,  $\text{GSD} = 1.8$ , interquartile range =  $3.44\text{--}8.03 \mu\text{m}$ ). About 85% of the aerosol particles had an aspect ratio of  $>3$ .

There are several ways to estimate the aerodynamic diameter ( $d_{\text{ae}}$ ) of fibers (reviewed in Fuchs<sup>(10)</sup> and Baron et al.<sup>(11)</sup>). Most of these utilized semi-empirical equations developed based on specific assumptions (infinitely long ellipsoidal particles, particular ranges of Reynolds numbers, and so on). The approach introduced by Fuchs (Formulas 23–46, 23–47 and 23–48 in Baron et al.)<sup>(11)</sup> seemed the least empirical and the most authentic, and was therefore applied in this study. This approach, when using the median length and assuming random orientation, produced a calculated median  $d_{\text{ae}}$  of  $1.73 \mu\text{m}$  with an interquartile range of  $1.71\text{--}1.74 \mu\text{m}$ .

The cumulative particle distribution is shown in Figure 3b to compare it with the cumulative distribution obtained for the particles in the generator suspension. Using the measured area density on the two filters (which agree to within 18%), and the flow rate and exposure time, we estimate the particle concentration in the chamber to be  $2.2 \times 10^4$  particles/L, which is in good agreement with the OPC determination. The background aerosol concentration in the chamber before the generation started was 340–430 particles/L. Thus, we believe that our subsequent filtration and leakage experiments were conducted in an atmosphere whose predominant contaminant is the deliberately introduced aerosol consisting mainly of elongated particles (i.e., fibers).

Monodisperse polystyrene particles with mean physical diameters of 1.01  $\mu\text{m}$  (PSI) and 1.54  $\mu\text{m}$  (PSII) (Bangs Laboratories Inc., Fishers, Ind.) were used to represent spherical particles. According to the manufacturer, the uncertainty in the size of PSII particles was 0.1  $\mu\text{m}$ ; the uncertainty for PSI was not given. Calculated mean aerodynamic diameters for PSI and PSII were 1.05 and 1.58  $\mu\text{m}$ , respectively. The latter is close to the aerodynamic size of fibers. PS particles were prepared at 1 wt.% in distilled water.

### Statistical Analysis

All statistical analysis was performed using SigmaPlot 12 (Systat Software Inc., San Jose, Calif.). Geometric means (GMs) and geometric standard deviations (GSDs) were used to describe filter and faceseal penetration data. Histograms and error bars for filter and faceseal penetrations (GM and GSD) were used to depict important results. Analyses of variance were performed separately for  $P_{\text{filter}}$  and  $P_{\text{faceseal}}$  as the dependent variable. A paired t-test was conducted to study the difference in penetrations between fibers vs. spherical particles measured at each breathing rate.

## RESULTS AND DISCUSSION

Filter penetration of fibers is compared with that of PSI ( $d_{\text{ae}} = 1.05 \mu\text{m}$ ) in Figure 4. Geometric means of filter penetration of fibers were 0.06, 0.09, and 0.08% at MIF of 15, 30, and 85 L/min, respectively. Corresponding values for PSI were 0.07, 0.12, and 0.12%, respectively. All filter penetrations of PSI were significantly higher than that of the fibers ( $p < 0.001$ ) at each breathing flow. This is consistent with the findings by Ortiz et al.<sup>(5)</sup> The filter penetration levels seen here are not surprising because NIOSH-certified N95-class FFRs undergo stringent filter testing as part of the certification process with capture  $>95\%$  of a charge neutralized sodium chloride particle challenge (mass median aerodynamic diameter =  $\sim 0.3 \mu\text{m}$ ) at a constant flow rate of 85 L/min.<sup>(12)</sup> The ratio of filter penetration for PSI to that of fibers varied from 1.1 to 1.5. Values for filter penetration of the fibers in this study were similar to ranges reported previously.<sup>(4-6)</sup>

Figure 5 shows the comparison of faceseal penetration between fibers and PSI at different breathing rates. Geometric means of faceseal penetration of fibers were 0.40, 0.14, and 0.09% at MIF of 15, 30, and 85 L/min, respectively. Corresponding values for PSI were 0.96, 0.41, and 0.17%, respectively. Faceseal penetrations for both types of particles were greater than the respective filter penetrations ( $p < 0.001$ ). This agrees with the previous findings reported by Cho et al.<sup>(7)</sup> and Grinshpun et al.,<sup>(8)</sup> indicating most penetration through respirators occurs through faceseal leakage. In this particular case, the above statement holds true even when the respirator is considered to have an acceptable seal (measured using fit testing instrumentation with fit factors  $> 100$ ). PSI showed 2.0–2.8 times higher faceseal penetration compared with fibers at the three breathing rates. This could be attributed to the increased interception of fiber vs. spherical particles, but the smaller  $d_{\text{ae}}$  of PSI particles could also contribute to this difference. However, the larger size PSII particles also had greater faceseal penetration than fibers. Faceseal penetrations of both particles decreased as breathing rate increased ( $p < 0.001$ ). This supports the finding in previous studies<sup>(7,13)</sup> and can be explained by greater effect of impaction and interception occurring at higher air velocities.

The GM of total penetration varied from 0.16% (for fibers at 85 L/min) to 1.03% (PSI at MIF = 15 L/min). In our previous field study,<sup>(14)</sup> which was conducted in agricultural environments using the same sampling setup and respirator model as in the current study, the GM of workplace protection factors was 124 for particles in the size range of 1–2  $\mu\text{m}$ . This corresponds to a penetration of 0.8%. Thus, the face seal leakage in the current study for PSI particles was comparable to those observed in the referred field study for particles of similar size. In contrast to many previous studies, in which fixed sized circular leaks have been used, our experimental setup has slit-type leaks located on the nose and chin. This sealing configuration was selected in our previous study to provide total penetration comparable to one observed in a field study.<sup>(7)</sup> Roberge et al.<sup>(15)</sup> have shown that nasal and cheekbone regions account for 71% of identified face seal leaks with three models of N95 FFRs. Furthermore, Oestenstadt and Bartolucci<sup>(16)</sup> showed that diffuse leaks are twice more common than point leaks. The experiments simulated respirator wearer exposure to elongated particles of various lengths, including fibers. However, only one respirator model and one manikin model were tested, which is a limitation of this study.

To elucidate the effect of aerodynamic size vs. shape on the observed differences, an additional experiment was conducted with the next largest available PS particle, PSII ( $d_{ae} = 1.58 \mu\text{m}$ ). In this experiment, an N95 FFR was tested at a MIF of 30 L/min. Figure 6 illustrates the comparison of penetration of particles with different aerodynamic diameters through filter medium and face seal leakage. Geometric means of filter penetration and face seal penetration of PSII were 0.14% and 0.36%, respectively. These values were close to the corresponding values (0.12 and 0.41%) for PSI ( $d_{ae} = 1.05 \mu\text{m}$ ) but significantly ( $p = 0.003$ ) higher than corresponding values for the fiber particles with the same diameter and  $d_{ae}$  of 1.73  $\mu\text{m}$  (0.09 and 0.14%). Filter and face seal penetration of fibers should be close to those obtained for PSII if the aerodynamic diameter is the dominant factor governing the particle deposition mechanisms. Filter and face seal penetration of fibers, however, were significantly lower than those of PSI and PSII. Moreover, the ratios of face seal penetration to filter penetration for fibers were 6.4, 1.6, and 1.1 at MIF of 15, 30, and 85 L/min. Corresponding values for PSI were 13.6, 3.3, and 1.5. This ratio was 2.6 for PSII at MIF of 30 L/min. This indicates that spherical particles penetrate more through face seal leakage compared with fibers, and the shape of the particles rather than the calculated aerodynamic diameter is a prevailing factor on deposition mechanisms through the tested respirator type. The results of this study cannot be extrapolated to smaller elongated particles, such as carbon nanotubes, which may have different behavior due to increased effects of diffusion and electrostatic forces.

## CONCLUSION

This study is unique in that it focuses on the comparison of face seal penetration of fibers and spherical particles. The experimental protocols simulated realistic workplace exposures where workers are exposed to elongated particles of various lengths, including fibers. The results show that spherical particles had 2.0–2.8 times higher face seal penetration compared with fibers. The difference in the filter penetration was smaller, below 1.5-fold. Filter penetration of the three different test particles were well below 5%, which is expected for NIOSH-certified N95 FFRs.

The results indicate that spherical particles had greater penetration through respirator filters and face seal leaks when compared with fibers of similar diameter. This difference was more pronounced for face seal leaks than for filter penetration, even for respirators considered to have an acceptable fit. The shape of the particles rather than the aerodynamic diameter is a prevailing factor on deposition mechanisms through the tested respirator type.

## Acknowledgments

This research was supported by the National Institute for Occupational Safety and Health (NIOSH R01 OH004085). Koken Ltd. (Tokyo, Japan) made the nebulizer and the breathing simulation system available to this study.

## References

1. Hinds, WC. *Aerosol Technology: Properties, Behavior, and Measurement of Airborne Particles*. New York: John Wiley & Sons, Inc; 1999.
2. Chen CC, Huang SH. The effects of particle charge on the performance of a filtering facepiece. *Am Ind Hyg Assoc J*. 1998; 59:227–233. [PubMed: 9586197]
3. Cheng Y-S, Powell QH, Smith SM, Johnson NF. Silicon carbide whiskers: Characterization and aerodynamic behaviors. *Am Ind Hyg Assoc J*. 1995; 56:970–978. [PubMed: 7572614]
4. Brosseau LM, Ellenbecker MJ, Evans JS. Collection of silica and asbestos aerosols by respirators at steady and cyclic flow. *Am Ind Hyg Assoc J*. 1990; 51:420–426. [PubMed: 2168122]
5. Ortiz LW, Soderholm SC, Valdez FO. Penetration of respirator filters by an asbestos aerosol. *Am Ind Hyg Assoc J*. 1988; 49:451–460. [PubMed: 3177224]
6. Cheng Y-S, Holmes TD, Fan B. Evaluation of respirator filters for asbestos fibers. *J Occup Environ Hyg*. 2006; 3:26–35. [PubMed: 16482975]
7. Cho KJ, Reponen T, McKay R, et al. Large particle penetration through N95 respirator filters and facepiece leaks with cyclic flow. *Ann Occup Hyg*. 2010; 54(1):68–77. [PubMed: 19700488]
8. Grinshpun SA, Haruta H, Eninger RM, Reponen T, McKay RT, Lee S-A. Performance of an N95 filtering facepiece respirator and a surgical mask during human breathing: Two pathways for particle penetration. *J Occup Environ Hyg*. 2009; 6:593–603. [PubMed: 19598054]
9. deAzevedo, D. [accessed October 7, 2012] Total inward leakage requirements for respirators. RIN 0920-AA33 (TSI comments regarding the CDC, HHS notice of proposed rulemaking). Available at <http://www.cdc.gov/niosh/docket/archive/docket137.html>
10. Fuchs, NA. *The Mechanics of Aerosols*. New York: Dover Publications, Inc; 1964.
11. Baron, PA.; Sorensen, CM.; Brockmann, JE. Nonspherical particle measurements: Shape factors, fractals, and fibers. In: Baron, PA.; Willeke, K., editors. *Aerosol Measurement: Principles, Techniques and Applications*. 2. New York: Wiley-Interscience; 2001.
12. National Institute for Occupational Safety and Health (NIOSH). *NIOSH Guide to the Selection and Use of Particulate Respirators*. Cincinnati, Ohio: DHHS, CDC, NIOSH; 1996. DHHS (NIOSH) Pub. no. 96–101
13. Chen CC, Ruuskanen J, Pilacinski W, Willeke K. Filter and leak penetration characteristics of a dust and mist filtering facepiece. *Am Ind Hyg Assoc J*. 1990; 51:632–639. [PubMed: 2270830]
14. Cho KJ, Jones S, Jones G, et al. Effect of particle size on respiratory protection provided by two types of N95 respirators used in agricultural settings. *J Occup Environ Hyg*. 2010; 7:622–627. [PubMed: 20835946]
15. Roberge RJ, Monaghan WD, Palmiero AJ, Shaffer R, Bergman MS. Infrared imaging for leak detection on n95 filtering facepiece respirators: A pilot study. *Am J Ind Med*. 2011; 54:628–636. [PubMed: 21594885]
16. Oestnstadt RK, Bartolucci AA. Factors affecting the location and shape of face leak sites on half-mask respirators. *J Occup Environ Hyg*. 2010; 7:332–341. [PubMed: 20379896]



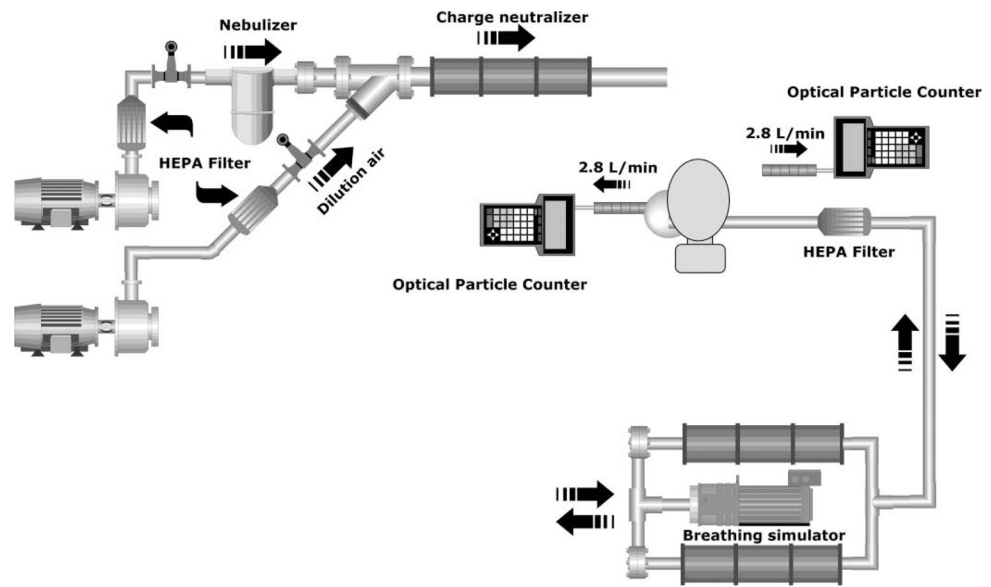


**FIGURE 1.**  
Schematic presentation of experimental setup.

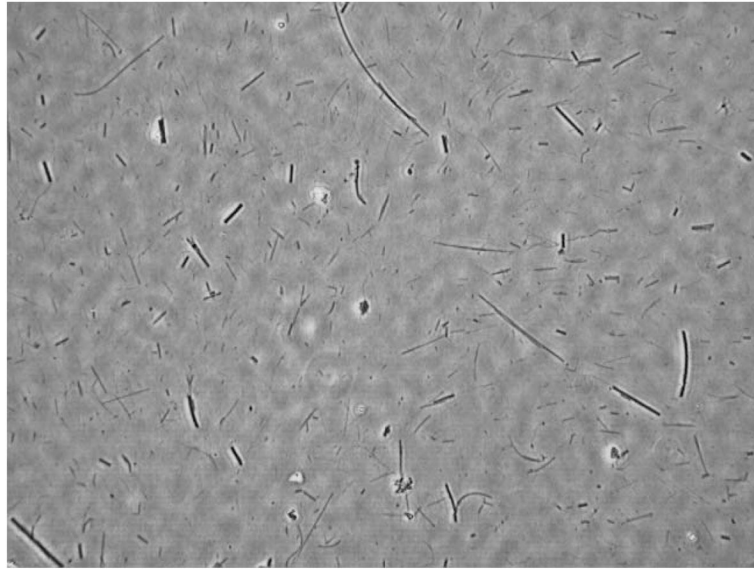


**FIGURE 2.** Optical microscopic image at 40× magnification for fibers collected on MCE filter. The total rectangular field of view is 200  $\mu\text{m}$  (vertical)  $\times$  250  $\mu\text{m}$  (horizontal). Note: Fibers orientated perpendicular to or nearly perpendicular to the focal plane will have a spherical appearance in this two-dimensional plane.

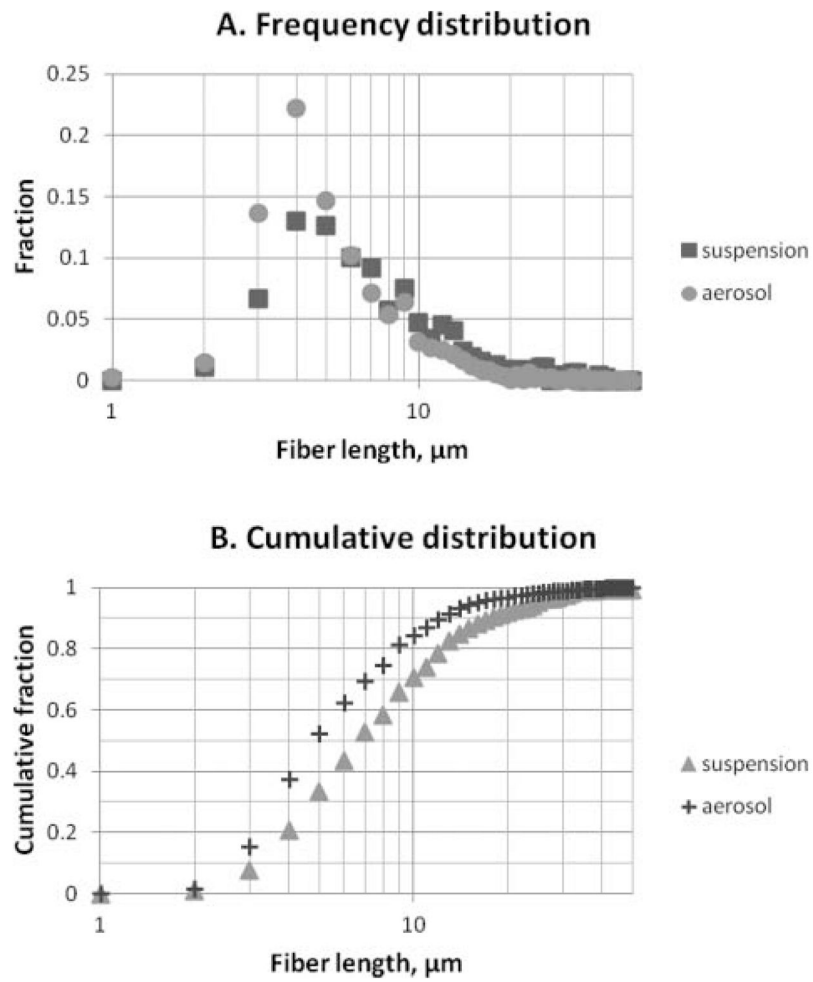


**FIGURE 3.** Distribution of the particle lengths in the generator suspension and in the test aerosol. Particles were collected on MCE filters and measured under a microscope: (a) frequency distributions, (b) cumulative distributions.

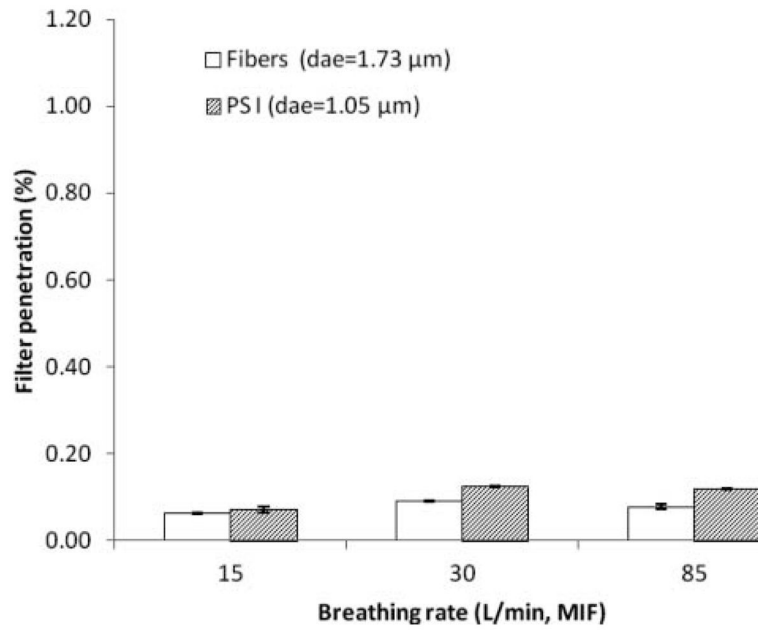


**FIGURE 4.** Comparison of filter penetration between fibers and PS particles at different breathing rates. The histograms present geometric means; error bars present geometric standard deviations.

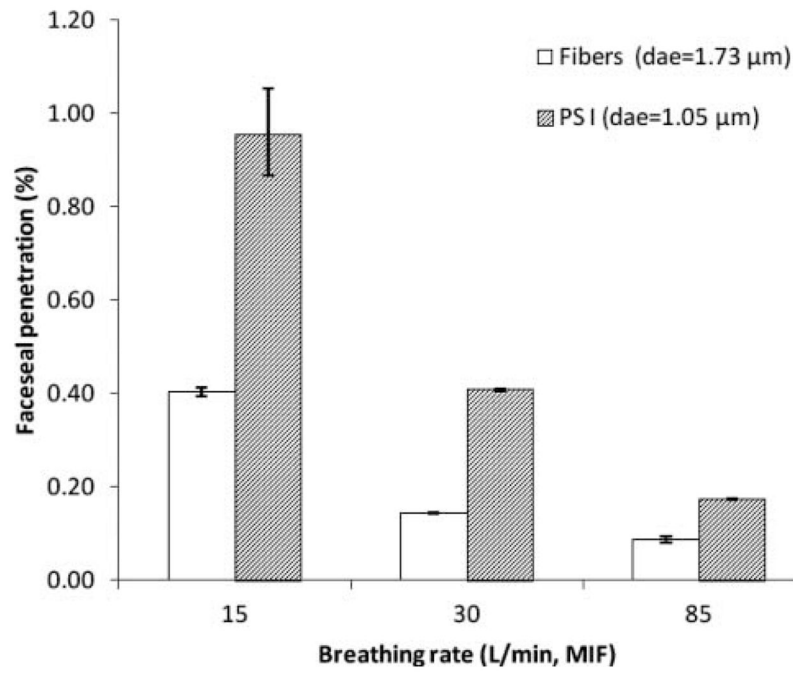


**FIGURE 5.** Comparison of face seal penetration between fibers and PS particles at different breathing rates. The histograms present geometric means; error bars present geometric standard deviations.

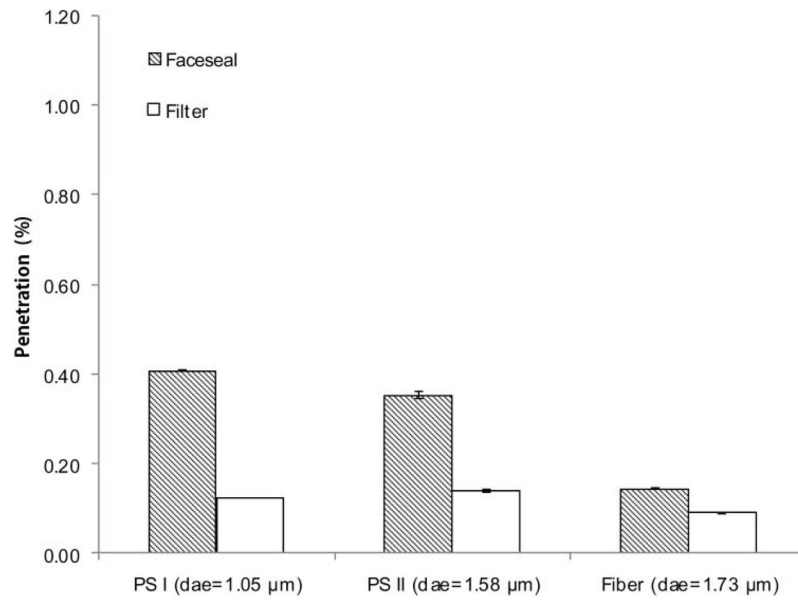


**FIGURE 6.** Comparison of penetrations of particles with different aerodynamic diameters at MIF of 30 L/min. The histograms present geometric means; error bars present geometric standard deviations.